Participation of the N-Terminal Region of Cε3 in the Binding of Human IgE to Its High-Affinity Receptor FcεRI†

Alistair J. Henry, Justin P. D. Cook, James M. McDonnell,‡ Graham A. Mackay, Jianguo Shi, Brian J. Sutton, and Hannah J. Gould*

The Randall Institute, King's College London, 26-29 Drury Lane, London, WC2B 5RL, United Kingdom

Received June 2, 1997; Revised Manuscript Received September 3, 1997⊗

ABSTRACT: The binding of immunoglobulin E (IgE) to its high-affinity receptor (FcεRI) expressed on mast cells and basophils is central to the development of an allergic reaction. Previous studies have implicated the third constant domain of IgE-Fc (Cε3) as the site of the interaction with FcεRI. We have prepared a series of site-directed mutants of human IgE-Fc, particularly focusing on the N-terminal "linker" region and AB loop of Cε3. The kinetics of binding IgE and its Fc fragments to the immobilized receptor were determined by surface plasmon resonance (SPR), and two phases of binding were observed. We identified one mutation in the N-terminal linker region, R334S, that has a dramatic effect on binding. R334S lowers the affinity of IgE-Fc for FcεRI by 120-fold, principally through an increase in the dissociation rate of the slower phase of the interaction. This mutation has a similar effect in Fcε3-4, a truncated form of IgE-Fc which lacks the Cε2 domain pair, and thus it does not exert its effect through altering the quaternary structure of IgE-Fc, firmly implicating Arg334 as a contact residue in the complex. However R334S has no effect on the binding of FcεRII (CD23), the low-affinity receptor for IgE, demonstrating the structural integrity of the mutated IgE-Fc. Circular dichroism spectroscopy and thermal stability studies further indicate that the R334S mutation does not disorder or destabilize the structure of IgE-Fc or Fcε3-4. These results demonstrate the importance of the N-terminal linker region of Cε3 in the interaction of IgE with FcεRI.

The binding of IgE to its high-affinity receptor (FcεRI)[1] expressed on mast cells and basophils, and subsequent receptor cross-linking by attachment of multivalent antigens, are essential early steps in the development of an allergic reaction. The resultant activation of these cells initiates an inflammatory cascade, which leads to the particular manifestations of allergy, depending on the site of allergen challenge. The IgE:FcεRI interaction is an obvious target for clinical intervention in the allergic response, and it has, therefore, long been the focus of studies to define the nature of the complementary binding sites in order to design competitive inhibitors that may be generally useful in the treatment of allergy (Sutton & Gould, 1993; McDonnell et al., 1996).

The Fc region of IgE consists of a dimer of the heavy-chain domains Cε2, Cε3, and Cε4, linked by two parallel interchain disulfide bonds at residues 241 and 328 in Cε2 [residue numbering according to Dorrington and Bennich (1978)]. Recombinant fragments of the Fc region, expressed in *Escherichia coli* (Helm et al., 1988, 1989, 1996), mammalian cells (Basu et al., 1993; Young et al., 1995; Shi et al., 1997), chimeric immunoglobulins (Baird et al., 1989; Weetal et al., 1990; Nissim & Eshhar, 1992; Nissim et al., 1991, 1993; Presta et al., 1994), mutants of IgE (Presta et al., 1994), and synthetic peptides (Stanworth et al., 1990; Nio et al., 1993) have all been used to define the site of interaction on IgE for FcεRI. These studies have indicated that the binding site is located within the Cε3 domain of IgE [reviewed in Gould (1993)]. It has been suggested that Cε4 may have a direct role in the interaction with FcεRI (Stanworth et al., 1990), but the available evidence is equally compatible with the possibility that it is required to maintain the active conformation of the Cε3 domain(s).

Attempts at further refinement of the FcεRI binding site have been contradictory. Site-directed mutagenesis of the IgE-Fc (Presta et al., 1994) has identified a number of discrete regions within Cε3 that are involved in FcεRI binding, namely the CD, FG, and EF loops in the predicted Ig domain structure of Cε3. This is at variance with a recent study using N- and C-terminally truncated peptides derived from human IgE-Fc (Helm et al., 1996), which highlights the AB loop as the main site of interaction with FcεRI. It is unclear from the latter study, however, whether the regions identified are directly involved in FcεRI binding or responsible for maintenance of the domain in an active conformation. The involvement of the "linker" region between Cε2

† This work was supported by Medical Research Council (U.K.) and National Asthma Campaign (U.K.) project grants to H.J.G. and B.J.S.

* Author to whom correspondence should be addressed: The Randall Institute, King's College London, 26-29 Drury Lane, London, WC2B 5RL, U.K.

‡ Present address: Laboratory of Physical Biochemistry, Rockefeller University, 1230 York Avenue, New York, NY 10021.

⊗ Abstract published in *Advance ACS Abstracts,* November 1, 1997.

[1] Abbreviations: CD, circular dichroism; cDNA, complementary DNA; Cε2, Cε3, Cε4, the three constant domains of IgE-Fc; ELISA, enzyme-linked immunosorbent assay; Fcε3-4, disulfide-linked dimer of Cε3-Cε4; FcεRI, high-afrfinity receptor for IgE; FcεRII, low-affinity receptor for IgE, CD23; FcγRI, IgG Fc-receptor type I, CD64; HBS, Hepes buffered saline; HPLC, high pressure liquid chromatography; IgE, immunoglobulin E; IgE-Fc, the Fc portion of IgE, Cε2-Cε3-Cε4; IgG, immunoglobulin G; IgG_4-Fc-$(sFc\varepsilon RI\alpha)_2$, fusion of IgG_4-Fc with sFcεRIα in place of the two Fab arms; PBS, phosphate buffered saline; PCR, polymerase chain reaction; RU, resonance unit; SDS−PAGE, sodium dodecyl sulfate-polyacrylamide gel electrophoresis; sFcεRIα, the extracellular domains of the α-chain of FcεRI; SPR, surface plasmon resonance; T_m, the mid-point of the thermal denaturation profile.

S0006-2960(97)01299-3 CCC: $14.00

and Cε3, particularly the stretch of amino acids between Asp330 at the junction of the domains and Gly335 within Cε3, in binding to FcεRI has been especially contentious, with authors advocating (Helm et al., 1988), or opposing (Helm et al., 1996; Nissim et al., 1993) its involvement or deciding that their data are inconclusive on the issue (Presta et al., 1994).

In the present study, we have examined the effect of a series of site directed mutations both on the binding of IgE-Fc to FcεRI and on the structure of the IgE-Fc. Mutations in the two debated regions, the linker region, and the AB loop were selected by inspection of the model of the structure of IgE-Fc (Padlan & Davies, 1986; Helm et al., 1991). Binding kinetics were measured by conventional cell binding assays and surface plasmon resonance (SPR). The information derived from these studies has enabled us to identify contact residues in the complex between IgE with FcεRI.

MATERIALS AND METHODS

(a) Site-Directed Mutagenesis. The human IgE-Fc [hIgE-Fc(N265Q,N371Q)] described by Young et al. (1995) was used as the basis for the mutagenesis of IgE-Fc. Single amino acid substitution in IgE-Fc was introduced using the PCR overlap extension method (Ho et al., 1989). Pairs of complementary oligonucleotide primers were used to define each mutation in IgE-Fc: D330SF 5′-GCGCATCTTC-CAACCCGAG, D330SR 5′-CGGGTTGGAAGATGCGAC; P333QF 5′-TCCAATCAGAGAGGGG, P333QR 5′-CCCCTCTCTGATTGGA; R334SF 5′-TCCAATC-CGAGCGGGGG, R334SR 5′-CCCCGCTCGGATTGGA; and R351EF 5′-CTGTTCATCGAGAAGTCGCCC, R351ER 5′-GGGCGACTTCTCGATGAACAG. The mutation in Fcε3-4 [a covalent dimer of the Cε3-Cε4 domains of IgE-Fc linked by Cys328 at the N-terminus of Cε3 described in Shi et al. (1997)] was introduced using a synthetic oligonucleotide primer to define the 5′ end of the construct including the *Eco*RV cloning site between the V-κ leader peptide cDNA and the Fcε3-4 cDNA, and another oligonucleotide primer was used to define the 3′ end of the mutated DNA fragment, downstream of the *Hpa*I in Cε3: RVR334SF 5′-ATTGATATCTGTGCAGATTCCAAC-CCGAGCGGGGTGAGC, RVR334SR 5′ CTCCGGCGTCG-CAAACGCATA. All mutations, and the integrity of the remaining sequence of the subcloned fragments, were confirmed by DNA sequencing using the chain termination method (Sanger et al., 1977). The mutated IgE-Fc constructs were subcloned into a pEE6-based expression vector which will support transient expression in CHO-L761h cells.

(b) Transient Expression of IgE-Fc and IgE-Fc Mutants. Initial screening of the IgE-Fc mutants for FcεRIα binding activity was performed using supernatants from transient transfection in CHO-L761h cells. Cells numbering 5×10^6 in 10 mL were transfected with 5 μg of plasmid DNA using the calcium phosphate precipitation method (Gorman, 1985). The supernatants were harvested after 3 days and concentrated 10-fold by ultrafiltration (Amicon). The yield of expressed protein was determined by IgE-specific ELISA, as described in Young et al. (1995). Initial kinetic analysis was performed by SPR without further purification.

(c) Isolation of Permanently Transfected Cell Lines and Protein Purification. The IgE-Fc DNA construct containing the R334S mutation was transfered to a pEE12-based expression vector which contains the glutamine synthetase cDNA as a selectable marker (Young et al., 1995). A stable NS-0 cell line of the R334S mutation in IgE-Fc was made, and the expressed protein purified as described before (Young et al., 1995).

The R334S mutation was introduced by PCR into Fcε3-4(N371Q) [described in Shi et al. (1997)]. The presence of the mutation was confirmed by DNA sequencing. Stable NS-0 cell lines were isolated, the expressed protein was purified on a IgG_4-Fc-$(sFc\epsilon RI\alpha)_2$ (Shi et al., 1997) affinity column, and its integrity was checked by HPLC and SDS−PAGE, as previously described.

(d) Measurement of Binding Kinetics. Assays were performed using SPR at 25 °C on a Pharmacia BIAcore instrument (Pharmacia Biosensor). A specific binding surface was prepared by coupling the IgG_4-Fc-$(sFc\epsilon RI\alpha)_2$ fusion protein to a CM5 sensor chip using the amine coupling kit according to the manufacturer's instructions, or by coupling the carbohydrate chains of sFcεRIα (Keown et al., 1995) to a CM5 sensor chip using the aldehyde coupling reaction, according to the manufacturer's instructions. Coupling density was restricted to less than 1000 RU. A parallel surface with IgG_4-Fc coupled at the same density as the IgG_4-Fc-$(sFc\epsilon RI\alpha)_2$ was also prepared in order to assess nonspecific binding. Samples of IgE-WT, (Burt et al., 1986, a myeloma protein purified as described for IgE-Fc), IgE-Fc, or Fcε3-4 and their mutants were diluted in HBS, pH 7.4, (supplied by Pharmacia Biosensor, being 10 mM Hepes, pH 7.4, 150 mM NaCl, 3.4 mM EDTA, and 0.005% surfactant P-20) and injected over the sensor chip at 5 μL/min. A 360 s association phase was followed by a 360 s dissociation phase. The sensor surface was regenerated by three 60 s pulses of 0.2 M glycine-HCl, pH 2.5. The data were analyzed using the BIAevaluation analysis package (version 2.1, Pharmacia Biosensor). Nonspecific binding was subtracted from the specific binding prior to kinetic analysis.

(e) Analysis of Binding Kinetics. The dissociation rate constant (k_d) for a monophasic model of binding was obtained by fitting the dissociation phase data to the following equation:

$$R = R_0 \, e^{-k_d(t-t_0)} \tag{1}$$

where R_0 is the response at the start of the dissociation and $t - t_0$ is the time function for the dissociation phase. The association rate constant (k_a) for a monophasic model of binding was obtained by fitting the association phase data to the following equation:

$$R = R_{eq}(1 - e^{-(k_a C n + k_d)(t-t_0)}) \tag{2}$$

where R_{eq} is the steady state response (binding at equilibrium, not necessarily reached in the sensorgram), k_a is the association rate constant, C is the molar concentration of the ligand, n is the steric interference factor which is set as 1 when the binding of one ligand does not block another binding site on the sensor surface, k_d is the dissociation rate constant, and $t - t_0$ is the time function for the association phase. The dissociation rate constants for a biphasic model of binding were obtained by fitting the dissociation phase data to the following equation:

$$R = R_1 e^{-k_{d1}(t-t_0)} + (R_0 - R_1) e^{-k_{d2}(t-t_0)} \tag{3}$$

where R_0 is the total response at the start of dissociation, R_1

is the contribution to R_0 from component 1 and $R_0 - R_1$ is the contribution to R_0 from component 2, $t - t_0$ is the time function for the dissociation phase, and k_{d1} and k_{d2} are the dissociation rate constants for the two components. The association rate constants for a biphasic model of binding were obtained by fitting the association phase data to the following equation:

$$R = R_{eq1}(1 - e^{-(k_{a1}Cn_1 + k_{d1})(t-t_0)}) + R_{eq2}(1 - e^{-(k_{a2}Cn_2 + k_{d2})(t-t_0)}) \quad (4)$$

where R_{eq1} and R_{eq2} are the steady state response levels (binding at equilibrium) for components 1 and 2, k_{a1} and k_{a2} are the association rate constants for components 1 and 2, C is the molar concentration of the ligand, $t - t_0$ is the time function for the association phase, and n_1 and n_2 are the steric interference factors for the two components, which are set at 1 when the binding of one component does not inhibit the binding at another ligand site.

The ability of the models to describe the experimental data was determined by examination of the residual plots, which were calculated by subtracting the experimental data points from the fitted curve. Residuals should be small and randomly distributed around zero. For the dissociation phase models, a further criterion was employed. The model allows the response after an infinite time of dissociation to be calculated, and clearly this should be zero. Fits that deviated in the estimation of this value by more than three times the noise value (i.e., 6 RU) were rejected.

The kinetics of IgE-Fc(R334S) binding to IgG_4-Fc-$(sFc\epsilon RI\alpha)_2$ were also analyzed using a BIAcore 2000 (Pharmacia Biosensor) to assess the apparant biphasicity. IgG_4-Fc-$(sFc\epsilon RI\alpha)_2$ (10 000 RU) was immobilized on all four sensor surfaces. IgE-Fc(R334S) was passed over the sensor surfaces, and the dissociated material collected in sequential 90 s windows during the dissociation phase. This was repeated 12 times in order to accumulate sufficient dissociated material for reanalysis. The collected fractions were concentrated 4−5 times using Centricon-30 centrifugal concentrators (Amicon), and their binding to IgG_4-Fc-$(sFc\epsilon RI\alpha)_2$ was analyzed by SPR.

(f) Circular dichroism. Circular dichroism (CD) measurements were performed on Jobin-Yvon (Longjumeau, France) CD6 spectrophotometer using cylindrical quartz cells of 0.05 cm path length. The spectrophotometer was calibrated for wavelength and ellipticity using *d*-10-camphorsulfonic acid. Samples were measured in the concentration range 100−500 μg/mL in 20 mM sodium phosphate, pH 7.4, at constant temperature in a thermostated cell holder.

Spectra were recorded in 0.2 nm steps with an integration time of 4 s and corrected by subtraction of the solvent spectrum obtained under identical conditions. The units of $\Delta\epsilon$ are inverse molarity centimeters per backbone amide.

Thermal stability was determined by heating the sample in PBS from 20 to 85 °C in 2 °C steps and measuring the ellipticity at 215 nm with a 30 s integration time. Ellipticity readings were normalized to calculate the fraction unfolded using the equation

$$F_u = \frac{\theta - \theta_N}{\theta_D - \theta_N} \quad (5)$$

where θ_N and θ_D represent the ellipticity values of fully folded and fully unfolded species at each temperature as calculated from the linear regression of the baselines preceding and following the transition region.

Position	Species		
	Human	Rat	Mouse
330	**Asp**	Asp	Asp
331	Ser	His	Asp
332	Asn	Glu	Glu
333	**Pro**	Pro	Pro
334	**Arg**	Arg	Arg
335	Gly	Gly	Gly
345	Pro	Pro	Pro
346	Phe	Leu	Leu
347	**Asp**	Asp	Asp
348	Leu	Leu	Leu
349	Phe	Tyr	Tyr
350	Ile	Gln	Gln
351	**Arg**	Asn	Asn
352	Lys	Gly	Gly

FIGURE 1: Comparison of the human, rat, and mouse protein sequences of the solvent accessible regions within the N-terminus of Cϵ3 (Asp330−Val361). The protein sequence of human (Max et al., 1982), rat (Steen et al., 1984), and mouse (Nishida et al., 1981) IgE were aligned, based on the homology with IgG-Fc (Deisenhofer, 1981). The alignment for the two regions 330−335 and 345−352 are shown, and the residues selected for mutagenesis are indicated in bold.

(g) Cell Binding Assays. The binding of IgE-Fc and Fcϵ3-4 to cell surface FcϵRI and FcϵRII was determined as described by Young et al. (1995).

RESULTS

(a) Selection of Mutations. Mutations were selected in order to examine the involvement of specific amino acids located in the N-terminal region of Cϵ3, comprising the N-terminal linker region and AB loop. Inspection of the molecular models of IgE-Fc (Padlan & Davies, 1986; Helm et al., 1991) indicates that only two portions of this region, Asp330-Gly335 in the linker region and the exposed residues of the AB loop from Pro345 to Ser353, are solvent accessible and, thus, available for FcϵRI binding. Within these two regions, residues that are conserved between human, mouse, and rat IgE were targeted for mutagenesis (Figure 1). Mouse and rat IgE are able to bind human FcϵRI, but human IgE is unable to bind rodent FcϵRI (Conrad et al., 1983). We, therefore, assumed that the residues in human IgE required for interaction with human FcϵRI are conserved in rodent IgE. On this basis, the mutations D330S, P333Q, R334S, and D347T were made in human IgE-Fc. In addition we generated R351E, also in human IgE-Fc, as its location within the solvent accessible region of the AB loop makes it a strong candidate for a contact residue if the AB loop is directly involved in the IgE:FcϵRI complex.

(b) Transient Expression and Kinetic Assays of IgE-Fc Mutants. The mutant IgE-Fcs were transiently expressed in CHO-L761h cells, and the levels of expression quantified by IgE-specific ELISA. Expression levels varied between different transfections, but usually fell within the range 150−400 ng/5 × 10^5cells/mL (data not shown).

Table 1: Summary of Association Rate Constants for the Binding of IgE-Fc Mutants to IgG_4-Fc-$(sFc\epsilon RI\alpha)_2$, as Determined by Surface Plasmon Resonance Using Transient Transfection Supernatants[a]

	association rate (M^{-1} s^{-1})				
analyte	experiment 1	experiment 2	experiment 3	experiment 4	mean
IgE-Fc[b]	$(4.3 \pm 1.1) \times 10^5$	$(3.1 \pm 1.2) \times 10^5$	$(2.3 \pm 1.9) \times 10^5$ [d]	ND[e]	$(2.5 \pm 1.0) \times 10^5$
IgE-Fc (tc)[c]	$(3.0 \pm 0.8) \times 10^5$	$(2.8 \pm 0.4) \times 10^5$	$(3.7 \pm 3.2) \times 10^5$	$(1.3 \pm 0.1) \times 10^5$	$(2.7 \pm 1.0) \times 10^5$
IgE-Fc(D330S)	$(2.0 \pm 0.6) \times 10^5$ [f]	$(8.1 \pm 2.7) \times 10^5$	$(8.4 \pm 6.0) \times 10^5$	$(1.2 \pm 0.1) \times 10^5$	$(4.9 \pm 3.8) \times 10^5$
IgE-Fc(P333E)	ND[e]	$(6.3 \pm 2.1) \times 10^5$ [g]	$(6.8 \pm 5.6) \times 10^5$	$(8.2 \pm 1.4) \times 10^5$	$(7.0 \pm 0.9) \times 10^5$
IgE-Fc(P333Q)	$(2.9 \pm 0.6) \times 10^5$	$(2.1 \pm 0.9) \times 10^5$	$(2.1 \pm 1.7) \times 10^5$	$(1.1 \pm 0.2) \times 10^5$	$(2.0 \pm 0.7) \times 10^5$
IgE-Fc(R334S)	$(2.3 \pm 0.2) \times 10^5$	$(4.7 \pm 2.2) \times 10^5$	$(3.8 \pm 3.2) \times 10^5$	$(1.1 \pm 0.1) \times 10^5$	$(2.9 \pm 1.6) \times 10^5$
IgE-Fc(R351E)	$(3.2 \pm 0.3) \times 10^5$	$(6.1 \pm 2.2) \times 10^5$	$(3.8 \pm 3.2) \times 10^5$	$(2.6 \pm 0.2) \times 10^5$	$(3.9 \pm 1.5) \times 10^5$

[a] Sensorgrams were analyzed using eq 2. The data for experiments 1 and 2 represent mean ± sd for five different ligand concentrations per sample, and those for experiments 3 and 4 represent mean ± sd for four different ligand concentrations per sample, unless otherwise stated. The overall mean for the association rates is given in the final column. [b] IgE-Fc wild-type purified from a permanently transfected NS-0 cell line (Young et al., 1995). [c] IgE-Fc wild-type (in which all the mutations are inserted) transiently transfected in CHO-L761h cells. [d] Data expressed as mean ± sd for five concentrations. [e] Not determined. [f] Data expressed as mean ± sd for four concentrations. [g] Data expressed as mean ± sd for three concentrations.

Table 2: Summary of Dissociation Rate Constants for the Binding of IgE-Fc Mutants to IgG_4-Fc-$(sFc\epsilon RI\alpha)_2$, as Determined by Surface Plasmon Resonance Using Transient Transfection Supernatants[a]

	dissociation rate (s^{-1})				
analyte	experiment 1	experiment 2	experiment 3	experiment 4	mean
IgE-Fc[b]	6.0×10^{-5}	5.1×10^{-5}	8.3×10^{-5}	ND[d]	$(6.5 \pm 1.6) \times 10^{-5}$
IgE-Fc (tc)[c]	4.7×10^{-5}	9.9×10^{-5}	3.1×10^{-5}	$(4.7 \pm 1.2) \times 10^{-5}$ [e]	$(5.6 \pm 2.9) \times 10^{-5}$
IgE-Fc(D330S)	3.0×10^{-5}	5.0×10^{-5}	6.3×10^{-5}	$(3.9 \pm 0.4) \times 10^{-5}$	$(4.6 \pm 1.4) \times 10^{-5}$
IgE-Fc(P333E)	ND[d]	2.1×10^{-4}	1.5×10^{-4}	$(2.9 \pm 0.6) \times 10^{-4}$ [e]	$(2.2 \pm 0.7) \times 10^{-4}$
IgE-Fc(P333Q)	3.4×10^{-5}	7.4×10^{-5}	7.4×10^{-5}	$(7.7 \pm 0.6) \times 10^{-5}$	$(6.5 \pm 2.0) \times 10^{-5}$
IgE-Fc(R334S)	1.5×10^{-3}	1.6×10^{-3}	1.9×10^{-3}	$(1.2 \pm 0.1) \times 10^{-3}$	$(1.5 \pm 0.3) \times 10^{-3}$
IgE-Fc(R351E)	1.6×10^{-5}	9.9×10^{-5}	6.4×10^{-5}	$(4.9 \pm 1.3) \times 10^{-5}$	$(5.7 \pm 3.4) \times 10^{-5}$

[a] Sensorgrams were analyzed using eq 1. For experiments 1−3, dissociation was measured only for the highest concentration of ligand. For experiment 4, dissociation was measured at all four concentrations of ligand, and the data given as mean ± sd for each data set. The overall mean ± sd is given in the last column. [b] IgE-Fc wild-type purified from a permanently transfected NS-0 cell line (Young et al., 1995). [c] IgE-Fc wild-type (in which all the mutations are inserted) transiently transfected in CHO-L761h cells. [d] Not determined. [e] Data expressed as mean ± sd for three concentrations.

Initial kinetic assays were performed by SPR with the receptor immobilized on the sensor surface in the form of the fusion protein IgG_4-Fc-$(sFc\epsilon RI\alpha)_2$. The association and dissociation phases of the response curve were fitted to monophasic models of association and dissociation. The mutant IgE-Fcs in supernatants from transiently transfected cells were compared with wild-type IgE-Fc, which was also obtained by transient transfection, and wild-type IgE-Fc, which was purified from an NS-0 cell line (Young et al., 1995). Tables 1 and 2 show the rate constants obtained from the data fitting for four separate experiments. The affinity constants derived from the rate constants are summarized in Table 3.

The SPR analysis indicates that wild-type IgE-Fc obtained by transient transfection has an association rate constant of $(2.7 \pm 1.0) \times 10^5$ M^{-1} s^{-1} and a dissociation rate constant of $(5.6 \pm 2.9) \times 10^{-5}$ s^{-1}, averaged over four experiments. These rates are in good agreement with the values obtained using purified IgE-Fc (Tables 1 and 2) and, therefore, indicate that the additional material present in the transient transfection supernatants did not affect the interaction with IgG_4-Fc-$(sFc\epsilon RI\alpha)_2$. None of the mutants had significantly different rates of association (Table 1). However, the IgE-Fc(P333E) and IgE-Fc(R334S) mutants had markedly faster dissociation rate constants [$(2.2 \pm 0.7) \times 10^{-4}$ s^{-1} and $(1.5 \pm 0.3) \times 10^{-3}$ s^{-1} respectively, averaged over four experiments, Table 2] when compared with wild-type IgE-Fc.

(c) Permanent Cell Lines of IgE-Fc(R334S) and Fcε3-4(R334S). The R334S mutation was inserted into IgE-Fc and Fcε3-4. The latter is a covalent dimer of the Cε3-Cε4 domains of IgE-Fc, linked by Cys328 retained from the C-terminal end of Cε2 in order to maintain the native proximity of the two ε-chains in the Cε2-Cε3 linker region. Permanent NS-0 cell lines of the mutant IgE-Fc and Fcε3-4 were made, and the expressed protein affinity purified from the tissue culture supernatants. Trace amounts of aggregated material were removed by gel filtration and the purity of the final material was demonstrated by analytical gel filtration (Figure 2). SDS−PAGE in reducing and nonreducing conditions was used to show that the interchain disulfide bonds were formed (data not shown). The recombinant protein fragments were homogeneous and monodisperse by both criteria.

Table 3: Summary of affinity constants for the binding of IgE-Fc mutants to IgG_4-Fc-$(sFc\epsilon RI\alpha)_2$, as Determined by Surface Plasmon Resonance Using Transient Transfection Supernatants[a]

analyte	affinity constant (M^{-1})
IgE-Fc[b]	$(5.4 \pm 2.3) \times 10^9$
IgE-Fc (tc)[c]	$(6.1 \pm 4.3) \times 10^9$
IgE-Fc(D330S)	$(9.8 \pm 5.9) \times 10^9$
IgE-Fc(P333E)	$(3.4 \pm 0.9) \times 10^9$
IgE-Fc(P333Q)	$(3.9 \pm 3.0) \times 10^9$
IgE-Fc(R334S)	$(1.8 \pm 0.9) \times 10^8$
IgE-Fc(R351E)	$(9.3 \pm 7.1) \times 10^9$

[a] The affinity constants for the IgE-Fc mutants were calculated from the association and dissociation rate constants that are shown in Tables 1 and 2. The affinity constant was determined for each ligand in each of the four reported experiments, and the mean ± sd for all experiments is shown. [b] IgE-Fc wild-type purified from a permanently transfected NS-0 cell line (Young et al., 1995). [c] IgE-Fc wild-type (in which all the mutations are inserted) transiently transfected in CHO-L761h cells.

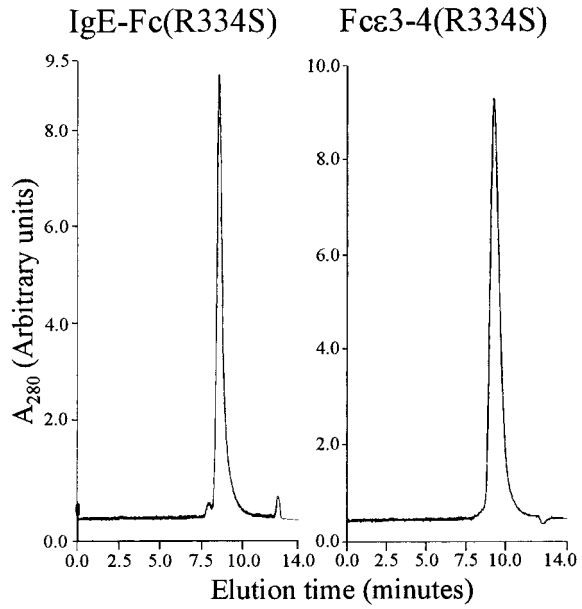

FIGURE 2: Gel filtration analysis of purified IgE-Fc(R334S) and Fcϵ3-4(R334S). Affinity purified IgE-Fc(R334S) and Fcϵ3-4(R334S) were further purified by gel filtration on a Zorbax GF-250 gel filtration column. The chromatograms demonstrate the homogeneity of material after the preparative gel filtration chromatography.

(d) Kinetic Analysis of IgE-Fc(R334S) and Fcϵ3-4(R334S) Binding to IgG_4-Fc-(sFcϵRIα)$_2$. The kinetics of binding were analyzed by SPR. The mutant proteins were compared with their unmutated counterparts and with IgE-WT. Figure 3 shows representative sensorgrams for all the proteins. Visual inspection of the sensorgrams for the wild-type and mutant IgE-Fc and Fcϵ3-4 indicates that the R334S mutation has a substantial effect upon the dissociation rates of these molecules from IgG_4-Fc-(sFcϵRIα)$_2$. Initially the data were fitted to a monophasic model of binding (as defined by eqs 1 and 2). Figure 4 shows representative fits for IgE-Fc and IgE-Fc(R334S) only. The other proteins assayed [IgE-WT, Fcϵ3-4, and Fcϵ3-4(R334S)] gave similar fits. It is evident from the size and nonrandom distribution of the residuals that a monophasic model (left-hand panels for both association and dissociation in Figure 4) does not adequately describe the observed interaction. The data were fitted to a biphasic model (right-hand panels in Figure 4), as described by eqs 3 and 4. The representative fits, along with the residual plots, for the biphasic model demonstrate that this model is a better description of the observed interaction. Similar results were obtained for IgE-WT, Fcϵ3-4, and Fcϵ3-4(R334S). Table 4 summarizes the rate constants derived from these fits for the purified proteins, IgE-WT, IgE-Fc, IgE-Fc(R334S), and the two mutants.

For the five proteins assayed [IgE-WT, IgE-Fc, IgE-Fc(R334S), Fcϵ3-4, and Fcϵ3-4(R334S)], the values for k_{a1} are identical to each other within experimental error. The values for k_{a2} are also within error of each other, except for Fcϵ3-4(R334S), which is ~20 times slower than the others. Striking differences are found in the dissociation rate constants, however, particularly k_{d2}. There are no differences between the dissociation rates of IgE-WT, IgE-Fc, and Fcϵ3-4, but IgE-Fc(R334S) and Fcϵ3-4(R334S) are markedly different from the wild-type protein fragments. For IgE-Fc(R334S), the value of k_{d2} is ~45 times higher than that of IgE-Fc (8.9×10^{-3} s^{-1} compared with 2.0×10^{-4} s^{-1}), and

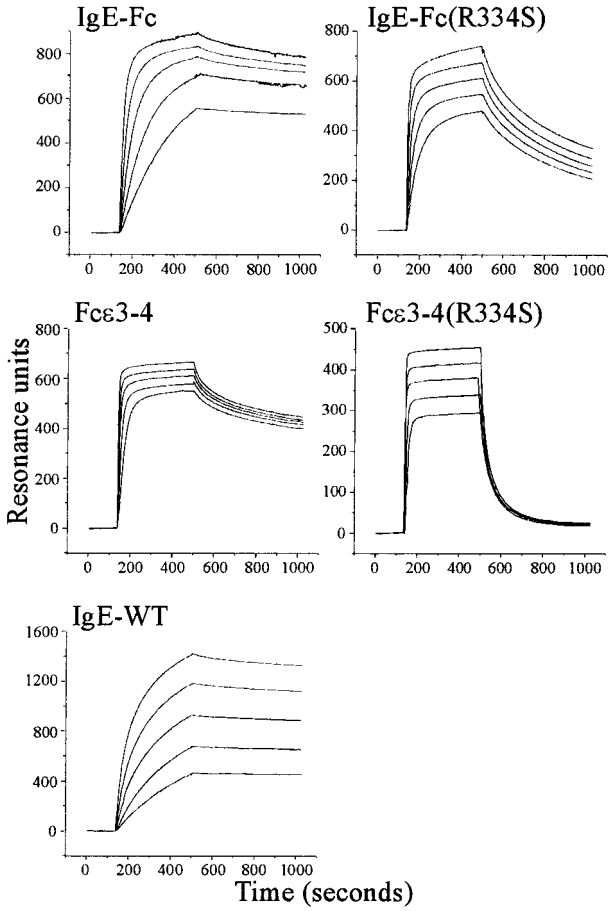

FIGURE 3: Sensorgrams of IgE-WT, IgE-Fc, IgE-Fc(R334S), Fcϵ3-4, and Fcϵ3-4(R334S) binding to immobilized IgG_4-Fc-(sFcϵRIα)$_2$. The binding of purified IgE-WT and IgE fragments was monitored by SPR. The different ligands were injected onto the sensor surface at five different concentrations in the range 15 nM to 2 μM. A 6 min association phase was followed by a 6 min dissociation phase with HBS buffer flowing over the sensor surface at 5 μL/min. Representative sensorgrams are shown.

the value of k_{d1} is ~5 times higher than that of IgE-Fc (4.6×10^{-2} s^{-1} compared with 1.0×10^{-2} s^{-1}). For Fcϵ3-4(R334S), the value of k_{d2} is ~250 times higher than that of Fcϵ3-4 (3.8×10^{-2} s^{-1} compared with 1.5×10^{-4} s^{-1}), although there is no significant difference in the k_{d1} values for the mutant and wild-type Fcϵ3-4. This increase in the second dissociation rate has a profound effect upon the affinity of the second component (K_{a2}), which is the component that dominates the observed interaction, reducing it to 1.0×10^7 M^{-1} and 6.8×10^6 M^{-1} for IgE-Fc(R334S) and Fcϵ3-4(R334S) respectively.

The kinetics of IgE-Fc(R334S) binding to FcϵRI were also determined by a cell binding assay. Table 5 summarizes the data obtained by this method, and it confirms the trend seen in the SPR assay, using transient transfection supernatants. In the cell binding assay the R334S mutation decreases the affinity of the interaction of IgE-Fc with FcϵRI, principally through a 12-fold increase in the dissociation rate [1.7×10^{-5} s^{-1} for wild-type IgE-Fc, compared with 2.0×10^{-4} s^{-1} for IgE-Fc(R334S), Table 5]; by SPR, the increase in dissociation rate was found to be 27-fold [5.6×10^{-5} s^{-1} for wild-type IgE-Fc, compared with 1.5×10^{-3} s^{-1} for IgE-Fc(R334S), Table 2]. The higher absolute values of the K_a determined by the cell binding assay [5.7×10^{10} M^{-1} for wild-type IgE-Fc, compared with 3.7×10^9 M^{-1} for IgE-Fc(R334S), Table 5], as compared with SPR [6.1×10^9 M^{-1}

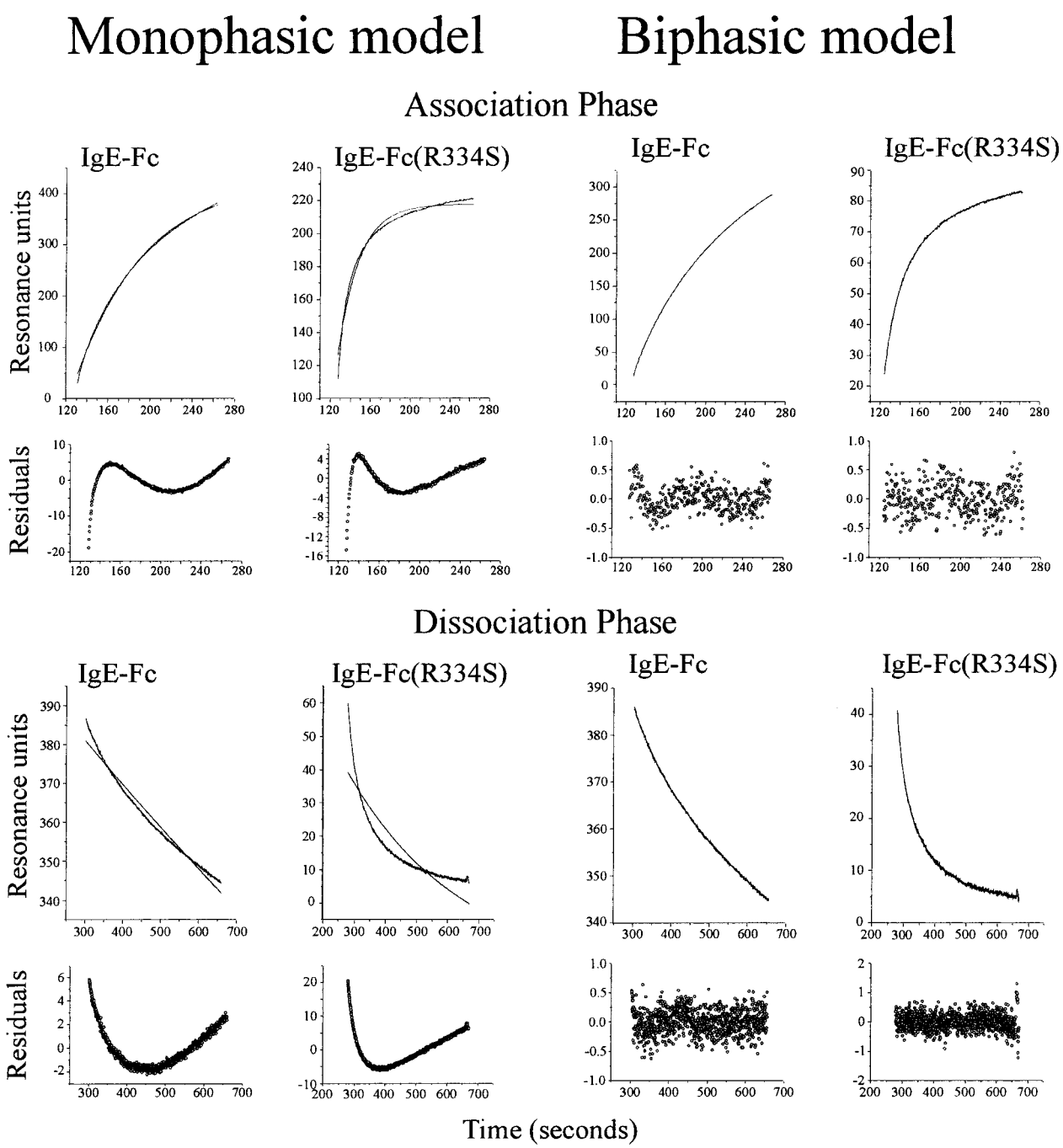

FIGURE 4: Fitting of SPR data for IgE-Fc and IgE-Fc(R334S) binding to immobilized IgG_4-Fc-$(sFc\epsilon RI\alpha)_2$. The association and dissociation phases of the interaction with IgG_4-Fc-$(sFc\epsilon RI\alpha)_2$ were fitted to monophasic (eqs 1 and 2) and biphasic (eqs 3 and 4) models of binding. The fitted lines are overlayed with the data in each plot. The residual plots (obtained by subtracting the calculated fit from the experimental data) are shown for each fit. Representative fits are shown for IgE-Fc at 125 nM and IgE-Fc(R334S) at 1000 nM.

for wild-type IgE-Fc and 1.8×10^8 M^{-1} for IgE-Fc(R334S), Table 3], will be discussed below.

(e) Analysis of Rebinding of IgE-Fc(R334S) to IgG_4-Fc-$(sFc\epsilon RI\alpha)_2$. We considered the possibility that the biphasic kinetics seen in the SPR assay might be a result of heterogeneity in the assayed ligand (IgE or IgE-Fc fragment). In order to test this possibility, IgE-Fc(R334S) was repeatedly injected over a sensor surface with immobilized IgG_4-Fc-$(sFc\epsilon RI\alpha)_2$ and the material that dissociated was collected in discrete time windows (Figure 5A). Each fraction was then reassayed for binding to IgG_4-Fc-$(sFc\epsilon RI\alpha)_2$. Figure 5B shows the fitted dissociation curves for the sequential fractions and Table 6 gives the dissociation rate constants and the R_1/R_0 ratios derived from these fits, for each fraction. It is clear that there is no difference between the fractions in either the ratio of the two binding components (R_1/R_0, Table 6) or their dissociation rate constants (k_{d1}, k_{d2}), and therefore, the biphasic kinetics do not result from heterogeneity in the assayed ligand.

(f) Binding of IgE-Fc(R334S) to FcεRII. IgE has a low-affinity receptor (FcεRII/CD23), with a completely different range of activities from FcεRI (Sutton & Gould, 1993; Gould et al., 1997) but which also binds to Cε3 (Vercelli et al., 1989; Nissim et al., 1993). The FcεRI and FcεRII binding sites on IgE appear to be located in different (although overlapping) parts of the protein (Helm et al., 1988, Vercelli et al., 1989; Nissim et al., 1993), and thus, the R334S mutation is not expected to have any direct effect upon the

Table 4: Summary of Kinetic Data for IgE-WT, IgE-Fc, IgE-Fc(R334S), Fcε3-4, and Fcε3-4(R334S) Binding to IgG_4-Fc-$(sFc\epsilon RI\alpha)_2$, as Determined by Surface Plasmon Resonance Using Purified Proteins[a]

	protein assayed				
constant	IgE-WT	IgE-Fc	IgE-Fc (R334S)	Fcε3-4	Fcε3-4 (R334S)
k_{a1} (M^{-1} s^{-1})	$(3.5 \pm 0.8) \times 10^5$	$(1.2 \pm 0.8) \times 10^6$	$(3.9 \pm 3.2) \times 10^5$	$(6.4 \pm 5.4) \times 10^5$	$(2.6 \pm 0.3) \times 10^5$
k_{a2} (M^{-1} s^{-1})	$(8.6 \pm 3.5) \times 10^4$	$(2.5 \pm 1.8) \times 10^5$	$(9.3 \pm 8.8) \times 10^4$	$(5.5 \pm 4.7) \times 10^4$	$(3.9 \pm 1.2) \times 10^3$
k_{d1} (s^{-1})	$(1.4 \pm 0.1) \times 10^{-2}$	$(1.0 \pm 0.1) \times 10^{-2}$	$(4.6 \pm 0.4) \times 10^{-2}$	$(1.7 \pm 0.1) \times 10^{-2}$	$(1.1 \pm 0.6) \times 10^{-2}$
k_{d2} (s^{-1})	$(3.6 \pm 1.9) \times 10^{-4}$	$(2.0 \pm 0.1) \times 10^{-4}$	$(8.9 \pm 0.4) \times 10^{-3}$	$(1.5 \pm 0.1) \times 10^{-4}$	$(3.8 \pm 0.6) \times 10^{-2}$
K_{a1} (M^{-1})[b]	2.5×10^7	1.1×10^8	8.6×10^6	3.8×10^7	3.4×10^5
K_{a2} (M^{-1})[c]	2.4×10^8	1.2×10^9	1.0×10^7	3.7×10^8	6.8×10^6
R_1/R_0	0.064 ± 0.001	0.043 ± 0.002	0.43 ± 0.03	0.029 ± 0.004	0.69 ± 0.06

[a] Sensorgrams were analyzed using eqs 3 and 4. Results are expressed as mean ± sd for five separate determinations. IgE-WT and IgE-Fc were measured in the concentration range of 15.6−250 nM, and all other proteins in the range 62.5−2000 nM. [b] Calculated as k_{a1}/k_{d1}. [c] Calculated as k_{a2}/k_{d2}.

Table 5: Summary of the Binding of IgE-Fc and IgE-Fc(R334S) to Cell Surface FcεRI[a]

	protein assayed	
constant	IgE-Fc	IgE-Fc(R334S)
k_a (M^{-1} s^{-1})	$(9.9 \pm 1.1) \times 10^5$ (4)	$(7.5 \pm 2.6) \times 10^5$ (4)
k_d (s^{-1})	$(1.7 \pm 0.2) \times 10^{-5}$ (7)	$(2.0 \pm 0.1) \times 10^{-4}$ (4)
K_a (M^{-1})[b]	5.7×10^{10}	3.7×10^9

[a] Results are expressed as mean ± sd for each assay. The numbers of experiments performed are given in parentheses. [b] Calculated as k_a/k_d.

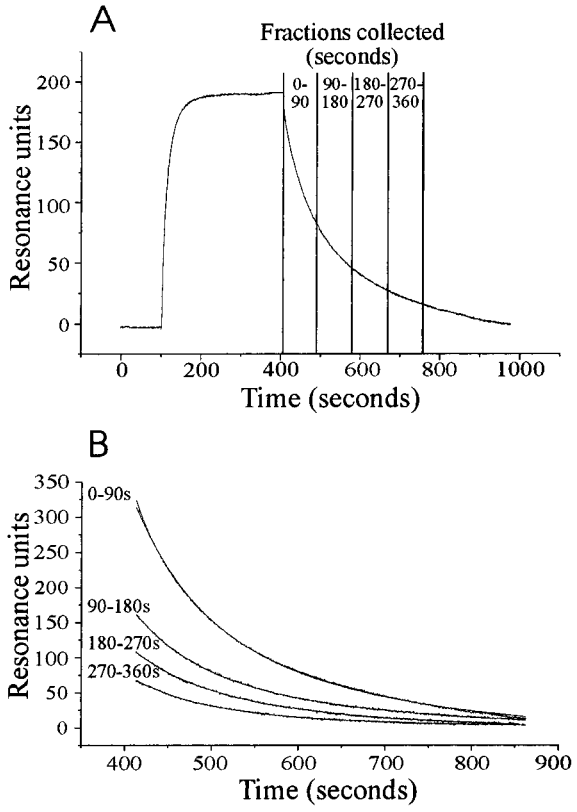

FIGURE 5: Rebinding to IgG_4-Fc-$(sFc\epsilon RI\alpha)_2$ of IgE-Fc(R334S) after dissociation from a IgG_4-Fc-$(sFc\epsilon RI\alpha)_2$ SPR sensor surface. IgE-Fc(R334S) that had dissociated from a sensor surface coated with IgG_4-Fc-$(sFc\epsilon RI\alpha)_2$ was collected and reanalyzed in order to determine whether the apparent biphasicity of binding was due to heterogeneity of the IgE-Fc(R334S). (Panel A) The four fractions that were collected as a function of the initial dissociation time. (Panel B) The reanalysis of the collected fractions using a biphasic model of dissociation (eq 3). The data and the fitted lines are shown for each fraction.

binding of IgE-Fc to FcεRII (Vercelli et al., 1989). Binding to FcεRII was used here only to assess the structural integrity of IgE-Fc(R334S). The data in Table 7 show that IgE-Fc and IgE-Fc(R334S) have identical affinities for FcεRII, implying that the R334S mutation does not have any gross effect upon the structure of the IgE-Fc.

Table 6: Summary of Dissociation Rate Data for Rebinding of IgE-Fc(R334S) to IgG_4-Fc-$(sFc\epsilon RI\alpha)_2$ by Surface Plasmon Resonance[a]

	constants		
fraction	k_{d1} (s^{-1})	k_{d2} (s^{-1})	R_1/R_0
unfractionated	0.016	4.9×10^{-3}	0.47
0−90 s	0.015	4.3×10^{-3}	0.45
90−180 s	0.015	5.5×10^{-3}	0.47
180−270 s	0.015	4.5×10^{-3}	0.45
270−360 s	0.013	4.9×10^{-3}	0.44

[a] The dissociation rate analysis was performed using the biphasic model (eq 3). Sequential 90 s fractions were collected as IgE-Fc(R334S) dissociated from immobilized IgG_4-Fc-$(sFc\epsilon RI\alpha)_2$, and reanalyzed for binding to IgG_4-Fc-$(sFc\epsilon RI\alpha)_2$ for comparison with the original, unfractionated material.

Table 7: Summary of Data for Binding of IgE-Fc and IgE-Fc(R334S) to Cell Surface FcεRII[a]

protein assayed	K_a (M^{-1})
IgE-Fc	$(3.2 \pm 2.4) \times 10^7$ (4)
IgE-Fc(R334S)	$(2.4 \pm 3.9) \times 10^7$ (4)

[a] Affinity is expressed as mean ± sd. Each individual experiment was performed in duplicate, and the number of repeat experiments is given in parentheses.

(g) Structural Analysis of IgE-Fc(R334S) and Fcε3-4(R334S). CD spectroscopy was also used to examine the conformation of the wild type and mutant IgE-Fc and Fcε3-4. Figure 6 shows the CD spectra of these molecules in the far UV region. Visual inspection of the spectra reveals no significant difference between the wild type and mutant proteins, and the spectra are in good agreement with those previously published for wild type proteins (Dorrington & Bennich 1978; Shi et al., 1997). The thermal stability of these protein fragments was also assessed by CD spectroscopy (Figure 7). Visual inspection of the denaturation curves indicates that the mutation does not affect the stability of the protein, and this is confirmed by the T_m value (mid point of thermal denaturation curves) for each protein studied (Table 8).

DISCUSSION

We set out to investigate the involvement of particular residues in the Cε3 domain of IgE in its interaction with FcεRI. Two regions were targeted: the N-terminal linker region and the loop between strands A and B. This was

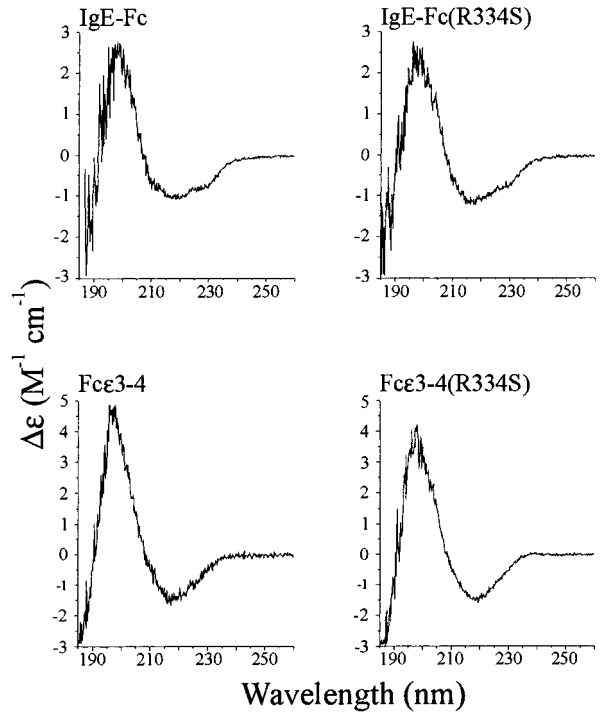

FIGURE 6: Circular dichroism spectra of IgE-Fc, Fcε3-4, IgE-Fc-(R334S), and Fcε3-4(R334S). All samples were measured at 400 μg/ml in 20 mM sodium phosphate buffer, pH 7.4, in a 0.5 mm path length cell at 4 °C.

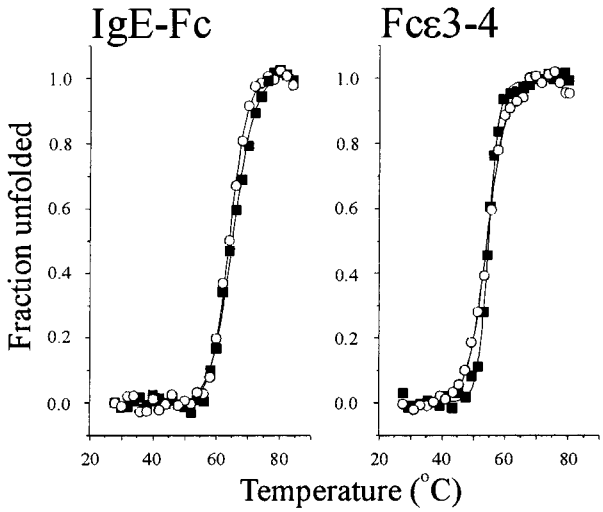

FIGURE 7: The thermal stability of IgE-Fc, IgE-Fc(R334S), Fcε3-4, and Fcε3-4(R334S), assessed by circular dichroism spectroscopy. The thermal denaturation profiles of wild-type (■) and mutant (○) IgE-Fc and Fcε3-4 were measured at 400 μg/mL in 20 mM sodium phosphate buffer, pH 7.4, and 150 mM NaCl. Samples were heated from 20 to 80 °C in 2 °C steps in a 0.5 mm path length cell, and the ellipticity at 215 nm was measured using a 32 s integration time. The change in ellipticity observed was transformed into fraction unfolded (F_u) as described in the Materials and Methods.

achieved by transient and permanent expression in mammalian cells of site-directed mutants of IgE-Fc and Fcε3-4, a subfragment of IgE-Fc consisting of a disulfide-linked dimer of the Cε3 and Cε4 domains. Transient expression of site-directed mutants of IgE-Fc yielded sufficient recombinant material to perform kinetic analysis of the interaction with FcεRIα by SPR. Before discussing the mutants, we note that the affinity constant determined by SPR for wild-type IgE-Fc binding to sFcεRIα is about 10 times lower than that derived by conventional cell binding assays [5.4×10^9 M^{-1} (Table 3) compared with 5.7×10^{10} M^{-1} (Table 5)]. This difference may reflect a requirement for membrane components in addition to FcεRIα, to confer high-affinity binding to FcεRI. It has been reported that the γ-chains of the IgG receptor, FcγRI, are required for high-affinity IgG binding (Miller et al., 1996). FcεRI utilizes the same γ-chains (Ravetch, 1994), and it is therefore possible that they are also essential for IgE to bind to its receptor with native affinity.

Table 8: T_m Values for Unfolding, Calculated from the Thermal Denaturation Profiles for IgE-Fc and Fcε3-4 and Their Respective Mutants

sample	T_m (°C)
IgE-Fc	64.6
IgE-Fc(R334S)	62.8
Fcε3-4	54.7
Fcε3-4(R334S)	54.5

Identification of a Contact Residue. The most dramatic result obtained with any of the mutants using transient transfection supernatants was with R334S. The K_a for FcεRI binding to this mutant was 34-fold lower than that of wild-type IgE-Fc (Table 3), and this lower affinity was mainly caused by a 27-fold increase in the dissociation rate constant (Table 2). This was confirmed by a cell binding assay which yields a 15-fold decrease in K_a, exclusively through an increase in the rate of dissociation (Table 5). These data suggest that Arg 334 is involved in the human IgE:FcεRI interaction. Interestingly, this is supported by an early observation that Arg365 in rat IgE [numbering according to Kabat et al. (1991) and the homologue of Arg334 in human IgE] is the trypsin cleavage site that is protected in the rat IgE:FcεRI complex (Perez-Montfort & Metzger, 1982).

We thus proceeded to make permanent cell lines expressing IgE-Fc(R334S) and the smaller fragment Fcε3-4(R334S). Kinetic analysis of the SPR data obtained with purified IgE-Fc and IgE-Fc(R334S) indicated that the interaction could only be adequately described by a biphasic model, as discussed in the following section. The even more striking effect of this mutation on the dissociation rate of the second component, namely a 45-fold increase in k_{d2}, leading to a 120-fold decrease in K_{a2} (Table 4), clearly indicates that Arg334 makes a major contribution to the interaction with FcεRIα.

Both IgE-Fc(R334S) and Fcε3-4(R334S) were analyzed by CD (Figure 6) and in thermal stability studies (Figure 7, Table 8) and were found to be indistinguishable from their wild-type counterparts. IgE-Fc(R334S) was also assayed for FcεRII binding (Table 7) and found to have the same affinity as wild-type IgE-Fc. By these criteria, the R334S mutation does not alter the gross structure of the Cε3 domain, and we therefore concluded that Arg334 is directly involved as a contact residue in the IgE-Fc:FcεRIα complex. Furthermore, the fact that the kinetic data for IgE-Fc(R334S) binding to FcεRIα derived by SPR is confirmed by the cell binding assay (Table 5) indicates that the mutation only affects the interaction of IgE-Fc with the α-chain of FcεRI and not with any of the accessory chains.

The effect of P333E on the dissociation rate (Table 2) confirms our previously published observations using a cell binding assay (Beavil et al., 1993). The observation that the P333Q mutation has no effect on the binding kinetics, however, suggests that Pro333 is not directly involved in the binding of IgE-Fc to FcεRIα. The increased dissociation

rate in the P333E mutation may result from unfavorable interactions between the glutamic acid residue and the surface of FcεRIα, implying that Pro333 must lie in close proximity to the receptor in the IgE:FcεRI complex.

In contrast to these mutations in the Cε2-Cε3 linker region, a mutation, R351E, located near Cε4 in the three-dimensional structure of IgE-Fc, had no effect on FcεRI binding. This is consistent with the results of Presta et al. (1994) who examined the mutation R351A. This residue lies in the loop region between the β-strands A and B of the Cε3 domain (the AB loop). Previous workers (Helm et al., 1996) found that Cε3 sequences truncated at either the N- or C-terminus of the AB loop lost FcεRI binding activity. Although they interpret their results to indicate that this loop is an essential part of the FcεRI binding site, it may be that its importance is rather as a determinant of an essential conformation at a distal contact site. We were unable to express the IgE-Fc-(D347T) mutant, even though multiple constructs were used. One possible explanation for this is that this mutation in the AB loop critically destabilized the structure of Cε3, prohibiting its accumulation and secretion.

Biphasic Nature of the Interaction. The SPR kinetic assays on the purified IgE-Fc, Fcε3-4, and their respective R334S mutants highlight additional features of the interaction of IgE with FcεRI that were not apparent in either the cell binding assay or the SPR assay with transient transfection supernatants. The SPR data measured with the purified proteins (Figure 3) could not be fitted by a simple monophasic interaction, and it was necessary to invoke a more complex, biphasic model. Fitting the SPR data to a biphasic model for both association and dissociation greatly improved the fits for both the wild-type and mutant IgE-Fc, as indicated by the residual plots (Figure 4); the same was observed for IgE-WT, Fcε3-4, and Fcε3-4(R334S) (data not shown). There are a number of potential explanations for the observed biphasicity of the binding kinetics for IgE-WT, IgE-Fc, and Fcε3-4 to sFcεRIα, which must be considered.

1. Heterogeneity of the Ligand. Gross heterogeneity, caused by aggregated material in the ligand sample, may be discounted by the results of the gel filtration analysis. Any remaining heterogeneity, including that due to heterogeneous or incomplete glycosylation, is not the cause of the biphasicity, as the rebinding experiments with IgE-Fc(R334S) (Figure 5, Table 6) indicate that there is no difference between material collected during the early and late phases of dissociation. This explanation can therefore be discounted.

2. Heterogeneity of the Immobilized Receptor. Two forms of the receptor [sFcεRIα and IgG_4-Fc-$(sFc\epsilon RI\alpha)_2$] and two entirely different means of coupling to the sensor surface (by primary amines and by carbohydrate), were used to measure the kinetics of IgE-Fc binding to FcεRIα. No difference between any of these combinations was detected in respect of the biphasic kinetics that are observed (data not shown). This makes it unlikely that it is the chemistry of immobilization that is responsible for the biphasic kinetics. Several different sensor surfaces have been prepared, and immobilized densities from 50 to 5000 RUs have been tested, and the biphasic kinetics are consistently observed on all surfaces. With nonspecific binding contributing to a maximum of 1% of the total binding, it cannot be nonspecific binding either that is responsible for the biphasicity.

3. Sequential Bivalent Attachment of the Ligand to the Receptor. Because of the symmetrical nature of IgE, it is theoretically possible that the biphasicity of binding represents a sequential monovalent to bivalent attachment of the IgE to the immobilized receptor. This explanation has to be discounted as the stoichiometry of binding of IgE, IgE-Fc, and Fcε3-4 to FcεRI has been shown to be 1:1 (Kanellopoulos et al., 1980; Robertson, 1993; Keown et al., 1995, 1997; Naito et al., 1996). We note that the magnitudes of the SPR signals at equilibrium (extrapolated from Figure 2) are consistent with a 1:1 stoichiometry of binding for IgE, IgE-Fc, and Fcε3-4. For example, 1000 RU of immobilized IgG_4-Fc-$(sFc\epsilon RI\alpha)_2$ (molecular mass 150 000 Da) would be expected to bind 1000 RU of IgE-Fc (molecular mass 75 000 Da) if each of the two sFcεRIα chains can bind one IgE-Fc fragment, and this is the value that we observe. The proportionally higher and lower RU values for IgE and Fcε3-4, respectively (Figure 3), are similarly consistent with a 1:1 stoichiometry of binding.

4. Diffusion of Ligand from the Sensor Matrix. The sensor surface is coated with a dextran matrix, through which the ligand must diffuse in order to bind to the immobilized receptor. The biphasicity of the dissociation phase could be due to diffusion of unbound ligand from within the sensor surface matrix (Edwards et al., 1995). This possibility can, however, be excluded by other results from this laboratory (Cook et al., 1997) in which immobilized site-directed mutants of sFcεRIα showed differences in *both* dissociation rate constants (k_{d1} or k_{d2}). If the faster dissociation component (with dissociation rate constant k_{d1}) is an artifact of diffusion of the ligand from the dextran matrix, then it should be unaffected by mutations in the immobilized receptor. It is clear that mutations in the receptor do affect k_{d1}, therefore, indicating that the faster dissociating component is not due to diffusion from the dextran matrix.

We, therefore, conclude that IgE (and IgE-Fc, Fcε3-4, and the R334S mutants) interact with FcεRI in a biphasic manner. We note, however, that our cell binding assay indicates that IgE-Fc interacts with FcεRI on the cell surface in a monophasic manner, and this has also been observed by others for the binding of rat IgE (Kulczycki & Metzger, 1974) and mouse IgE (Wank et al., 1983) to FcεRI on RBL cells. However, this is to be expected because of the experimental limitations of this type of assay. It is impossible to take accurate measurements of either association or dissociation within the first few minutes of the reaction because of the time that it takes to process the samples. Thus, the contribution of any fast component cannot be measured in this assay, and the reaction appears to be monophasic. No evidence for biphasic kinetics was apparent in the data derived from the transient transfection supernatants either, as reported in this paper. This is a result of the low concentration of specific ligand (IgE-Fc) within the supernatants, for which the signal to noise ratio is too low to unambiguously define the two phases.

The biphasic interaction is characterized by a higher affinity component, defined by k_{a2}, k_{d2}, and K_{a2}, and a lower affinity component, defined by k_{a1}, k_{d1}, and K_{a1} (Table 4), and it is the higher affinity component which dominates the interaction. The R334S mutation in IgE-Fc has very little effect upon the association rate of either component, but a large effect on the second dissociation rate constant (k_{d2}, Table 4); it is a 45-fold enhancement in this dissociation rate constant for IgE-Fc(R334S) that is primarily responsible for the 120-fold reduction in K_{a2}. This would suggest that Arg334 is not involved in the initial complex formation, but

is essential for the formation of a high-affinity complex.

Arg334 and the Bending of IgE-Fc. In view of the location of Arg 334 in the model of IgE-Fc (Padlan & Davies, 1986; Helm et al., 1991, and see Figure 8), it is possible that the R334S mutation could have an effect upon the quaternary structure of the Fc by altering the disposition of the Cε2 domains relative to Cε3. It is known that both IgE (Davis et al., 1990; Zheng et al., 1991; A. Beavil, S. Perkins, & B. Sutton, unpublished data) and IgE-Fc (Beavil et al., 1995) are bent in solution, and that in IgE-Fc the bend is most likely to occur between Cε2 and Cε3 (Beavil et al., 1995). Mutation of Arg 334 could therefore affect the bend in the IgE-Fc and hence access to a site in Cε3. It was for this reason that we introduced the R334S mutation into Fcε3-4, which lacks the Cε2 domains. [A similar mutation in IgE, which did cause a reduction in binding, was uninterpretable on account of this problem (variant 64; Presta et al., 1994)]. The results show clearly that the mutation is equally, if not more, effective in Fcε3-4 than IgE-Fc in reducing the affinity of the interaction with FcεRIα (Table 4). As with IgE-Fc, this reduction in the affinity was principally determined by an increase in the dissociation rate, which in Fcε3-4 is enhanced by ~250-fold for k_{d2} by this mutation. We, therefore, conclude that the R334S mutation does not exert its effect by changing the quaternary structure of IgE-Fc, but is directly involved in the interaction with FcεRIα.

An Extensive Binding Interface. In an earlier study, a number of residues (Arg376, Ser378, Lys380, Glu414, Arg427, and Met430) in the CD, EF, and FG loops of Cε3 were found to reduce FcεRI binding by up to 9-fold when mutated in IgE, as determined in a qualitative cell binding assay (Presta et al., 1994). However, Arg334 is located on the opposite face of the predicted three-dimensional structure of Cε3 from those residues proposed by Presta et al. This paradox is resolved when it is appreciated that in the predicted structure of IgE-Fc, two Cε3 domains are related by a 2-fold axis of symmetry, so that the opposite faces of Cε3 are presented on the same side of IgE-Fc, one face from each Cε3 domain (Figure 8). One further residue that affects FcεRI binding was identified by Presta et al. (1994), Arg393, and it lies on the same face as Arg334. All the mutations thus identified define a continuous contact surface for FcεRI comprised of amino acids distributed between the two Cε3 domains.

Such a large interaction surface in IgE-Fc implies the participation of both extracellular domains of FcεRIα, since the distance between the α-carbons of Arg393 and Lys380 is ~3.8 nm (Figure 8), and the maximum dimension of one α-chain domain is only ~3.0 nm. While the membrane-proximal α(2) domain of FcεRIα has been shown to exhibit IgE binding (Mallamaci et al., 1993; Robertson, 1993; Scarselli et al., 1993) and various determinants of IgE binding have been mapped to this domain [reviewed in Hulett and Hogarth (1994) and McDonnell et al. (1996)], the isolated α(2) domain is significantly less active than the whole extracellular portion (Robertson, 1993, Scarselli et al., 1993), implying a role for the α(1) domain. This issue will be discussed further in the following paper in this issue.

This definition of an extended region of IgE involved in the interaction with FcεRI allows a physical explanation of the biphasic kinetics to be proposed. The lower affinity component of the biphasic interaction (defined by k_{a1}, k_{d1}, and K_{a1}) may represent the formation of a short-lived, low-affinity, complex which is mediated by some, or all, of the

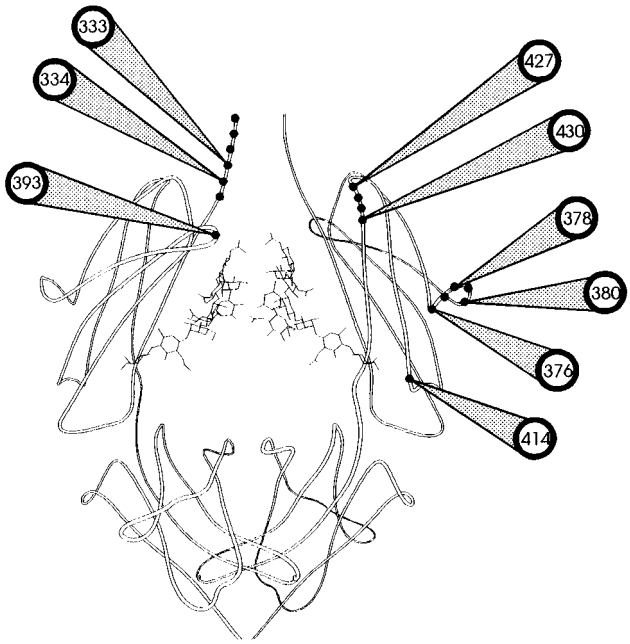

FIGURE 8: Schematic representation of the positions of residues in the Cε3 domains of IgE-Fc implicated in FcεRI binding. The positions of residues Arg376, Ser378, Lys380, Glu414, Arg427, Met430, and Arg393 (Presta et al., 1994), Pro333 and Arg334 are identified on a ribbon diagram of Fcε3-4; the model is based on Padlan and Davies (1986).

residues identified by Presta et al. (1994). Formation of the long-lived, high-affinity complex (characterized by k_{a2}, k_{d2}, and K_{a2}) may involve engagement of all the residues that constitute the binding site on both Cε3 domains, including Arg334, mutation of which we know dramatically affects only k_{d2} and K_{a2}. The importance of Arg334 to this high-affinity complex is evident by its contribution of 23% of the binding energy of the IgE-Fc:sFcεRIα complex.[2] This two-phase model is currently being tested by detailed kinetic analysis of the mutants defined by Presta et al. (1994).

Comparison with IgG:Receptor Interactions. The structurally homologous position to Arg334 in IgG (residue 236) is adjacent to the first residue to be identified as critical for the binding of IgG_{2a} to FcγRI, namely Leu235 (Duncan et al., 1988). Residues Leu234 to Gly237 have been shown to be important in IgG_1 (Lund et al., 1991) and IgG_3 (Chappel et al., 1991) binding to FcγRI and also FcγRII (Lund et al., 1991). Furthermore, residues Arg427 and Met430 identified by Presta et al. (1994) lie within the "hinge-proximal bend" (FG loop), the homologous residues to which in IgG_1 and IgG_3 have been shown to be important in IgG:FcγRI interactions (Woof et al., 1986; Canfield & Morrison, 1991; Chappel et al., 1993). It appears, therefore, that IgE interacts with FcεRI through a region that is structurally homologous to a receptor binding region of IgG. However, the IgG:FcγR interactions may be restricted to the hinge and hinge-proximal bends of IgG (Duncan et al., 1988; Chappel et al., 1991; Lund et al., 1991), whereas the IgE:FcεRI interaction appears to involve a greater surface area. This may account for the exceptionally high affinity of the IgE:FcεRI interaction, which is 1−2 orders of magnitude greater than that for any other Ig:FcR interaction (Ravetch & Kinet, 1991).

In conclusion, we have demonstrated the importance of Arg334 for the binding of IgE to FcεRI, but not to FcεRII,

[2] The contribution of Arg334 to the overall ΔG is calculated as $1 - [\ln K_{a2}(\text{Arg334})]/[\ln K_{a2}(\text{wt})]$.

delineated a large contact region on IgE-Fc that spans both Cε3 domains and proposed an explanation for the observed biphasic nature of the kinetics of this interaction. Understanding the precise contributions of individual residues to the kinetics of binding and dissociation may be exploited in the design of inhibitory compounds for the clinical management of allergic disease.

ACKNOWLEDGMENT

We thank Pharmacia Biosensor for the use of a BIAcore 2000 biosensor for the rebinding experiments, and Dr. Peter Steffner for helpful discussion of the kinetic analysis. IgE-WT was a kind gift of Dr D. Stanworth, Birmingham University, U.K.

REFERENCES

Baird, B., Shopes, R. J., Oi, V. T., Erickson, J., Kane, P., & Holowka, D. (1989) *Int. Arch. Allergy Appl. Immunol. 88*, 23−28.

Basu, M., Hakimi, J., Dharm, E., Kondas, J. A. Tsien, W.-H., Pilson, R. S., Lin, P., Gilfillan, A., Haring, P., Braswell, E. H., Nettleton, M. Y., & Kochan, J. P. (1993) *J. Biol. Chem. 269*, 13118−13127.

Beavil, A. J., Beavil, R. L., Chan, C. M. W., Cook, J. P. D., Gould, H. J., Henry, A. J., Owens, R. J., Shi, J., Sutton, B. J., & Young, R. J. (1993) *Biochem. Soc. Trans. 21*, 968−972.

Beavil, A. J., Young, R. J., Sutton, B. J., & Perkins, S. J. (1995) *Biochemistry 34*, 14449−14461.

Burt, D. S., Hastings, G. Z., & Stanworth, D. R. (1986) *Mol. Immunol. 23*, 181−191.

Canfield, S. M., & Morrison, S. L. (1991) *J. Exp. Med. 173*, 1483−1491.

Chappel, M. S., Iseman, D. E., Everett, M., Xu, Y. Y., Dorrington, K. J., & Klein, M.H. (1991) *Proc. Natl. Acad. Sci. U.S.A. 88*, 9036−9040.

Chappel, M. S., Isenman, D. E., Oomen, R., Xu, Y. Y., & Klein, M. H. (1993) *J. Biol. Chem. 268*, 25124−25131.

Conrad, D. H., Wingard, J. R., & Ishizaka, T. (1983) *J. Immunol. 130*, 327−333.

Cook, J. P. D., Henry, A. J., McDonnell, J. M., Owens, R. J., Sutton, B. J., & Gould, H. J. (1997) *Biochemistry 36*, 15579−15588.

Davis, K. G., Glennie, M., Harding, S. E., & Burton, D. R. (1990) *Biochem. Soc. Trans. 18*, 935−936.

Deisenhofer, J. (1981) *Biochemistry 20*, 2361−2370.

Dorrington, K. J., & Bennich, H. H. (1978) *Immunol. Rev. 41*, 3−25.

Duncan, A. R., Woof, J. M., Partridge, L. J., Burton, D. R., & Winter, G. (1988) *Nature 332*, 563−564.

Edwards, P. R., Gill, A., Pollard-Knight, D. V., Hoare, M., Buckle, P. E., Lowe, P. A., & Leatherbarrow, R. J. (1995) *Anal. Biochem. 231*, 210−217.

Gorman (1985) in *DNA cloning* (Glover, Ed.) Vol. II, pp 143−190, Academic Press.

Gould, H. (1993) in *The genetics of asthma* (Marsh, D. G., Cockhart, A., & Holgate, S. T., Eds.) pp 309−321, Blackwell Scientific Publications, London.

Gould, H. J., Beavil, R. L., Reljić, R., Shi, J., Ma, C., Sutton, B. J., & Ghirlando, R. (1997) in *Molecular mechanisms of IgE regulation* (Vercelli, D., Ed.) John Wiley & Sons Ltd., Chichester, U.K., in press.

Helm, B., Marsh, P., Vercelli, D., Padlan, E., Gould, H., & Geha. R. (1988) *Nature 331*, 180−183.

Helm, B., Kebo, D., Vercelli, D., Glovsky, M. M., Gould, H., Ishizaka, K., Geha, R., & Ishizaka, T. (1989) *Proc. Natl. Acad. Sci. U.S.A. 86*, 9465−9469.

Helm, B. A., Ling, Y., Teale, C., Padlan, E. A., & Brüggemann, M. (1991) *Eur. J. Immunol. 21*, 1543−1548.

Helm, B. A., Sayer, I., Higginbottom, A., Cantarelli-Machado, D., Ling, Y., Ahmad, K., Padlan, E. A., & Wilson, A. P. M. (1996) *J. Biol. Chem. 271*, 7494−7500.

Ho, S. N., Hunt, H. D., Horton, R. M., Pullen, J. K., & Pease, L. R. (1989) *Gene. 77*, 51−59.

Hulett, M. D., & Hogarth, P. M. (1994) *Adv. Immunol. 57*, 1−127.

Kabat, E. A., Wu, T. T., Reid-Miller, M., Perry, H. M., & Gottesman, K. S. (1991) *Sequences of Proteins of Immunological Interest.*, 5th ed., U.S. Department of Health and Human Services.

Kanellopoulos, J. M., Liu, T. Y., Poy, G., & Metzger, H. (1980) *J. Biol. Chem. 255*, 9060−9066.

Keown, M. B., Ghirlando, R., Young, R. J., Beavil, A. J., Owens, R. J., Perkins, S. J., Sutton, B. J., & Gould, H. J. (1995) *Proc. Natl. Acad. Sci. U.S.A. 92*, 1841−1845.

Keown, M. B., Ghirlando, R., Mackay, G. A., Sutton, B. J., & Gould, H. J. (1997) *Eur. Biophys. J. 25*, 471−476.

Kulczycki, A., & Metzger, H. (1974) *J. Exp. Med. 140*, 1676−1695.

Lund, J., Winter, G., Jones, J. T., Pound. J., Tanaka,. T., Walker, M. R., Artymiuk, P. J., Arata, Y., Burton, D. R., Jefferis, R., & Woof, J. M. (1991) *J. Immunol. 147*, 2657−2662.

Mallamaci, M. A., Chizzonite, R., Griffen, M., Nettleton, M., Hakimi, J., Tsien, W.-H., & Kochan, J.-P. (1993) *J. Biol. Chem. 268*, 22076−22083.

Max, E. E., Battey, J., Ney, R., Kirsch, I. R., & Leder, P. (1982) *Cell 29*, 691−699.

McDonnell, J. M., Beavil, A. J., Mackay, G. A., Jameson, B. A., Korngold, R., Gould, H. J., & Sutton, B. J. (1996) *Nat. Struct. Biol. 3*, 419−426.

Miller, K. L., Duchemin, A.-M., & Anderson, C. L. (1996) *J. Exp. Med. 183*, 2227−2233.

Naito, K., Hirama, M., Okumura, K., & Ra, C. (1996) *J. Allergy Clin. Immunol. 97*, 773−780.

Nio, N., Seguro, K., Ariyoshi, Y., Imano, K., Yakuo, I., Kita, A., & Nakamura, H. (1993) *FEBS Lett. 319*, 225−228.

Nishida, Y., Kataoka, T., Ishida, N., Nakai, S., Kishimoto, T., Bottcher, I., & Honjo, T. (1981) *Proc. Natl. Acad. Sci. U.S.A. 78*, 1581−1585.

Nissim, A., & Eshhar, Z. (1992) *Mol. Immunol. 29*, 1065−1072.

Nissim, A., Jouvain, M.-H., & Eshhar, Z. (1991) *EMBO J. 10*, 101−107.

Nissim, A., Schwarzbaum, S., Siraganian, R., & Eshhar, Z. (1993) *J. Immunol. 150*, 1365−1374.

Padlan, E. A., & Davies, D. R. (1986) *Mol. Immunol. 23*, 1063−1075.

Perez-Montfort, R., & Metzger, H. (1982) *Mol. Immunol. 19*, 1113−1125.

Presta, L., Shields, R., O'Connell, L., Lahr, S., Porter, J., Gorman, C., & Jardieu, P. (1994) *J. Biol. Chem. 269*, 26368−26373.

Ravetch, J. V. (1994) *Cell 78*, 553−560.

Ravetch, J. V., & Kinet, J.-P. (1991) *Annu. Rev. Immunol. 9*, 457−492.

Robertson, M. W. (1993) *J. Biol. Chem. 268*, 12736−12743.

Sanger, F., Nicklen, S., & Coulsen, A. (1977) *Proc. Natl. Acad. Sci. U.S.A. 74*, 5463−5467.

Scarselli, E., Esposito, G., & Traboni, C. (1993) *FEBS Letts. 329*, 223−226.

Shi, J., Ghirlando, R., Beavil, R. L., Beavil, A. J., Keown, M. B., Young, R. J., Owens, R. J., Sutton, B. J., & Gould, H. J. (1997) *Biochemistry 36*, 2112−2122.

Stanworth, D. R. Jones, V. M., Lewin, I. V., & Nayyar, S. (1990) *Lancet 336*, 1279−1281.

Steen, M. L., Hellman, L., & Pettersson, U. (1984) *J. Mol. Biol. 177*, 19−32.

Sutton, B. J., & Gould, H. J. (1993) *Nature 366*, 421−428.

Vercelli, D., Helm, B., Marsh, P., Padlan, E., Geha, R. S., & Gould, H. J. (1989) *Nature 338*, 649−650.

Wank, S. A., Delisi, C., & Metzger, H. (1983) *Biochemistry 22*, 954−959.

Weetall, M., Shopes, B., Holowka, D., & Baird, B. (1990) *J. Immunol. 145*, 3849−3854.

Woof, J. M., Partridge, L. J., Jefferis, R., & Burton, D. R. (1986) *Mol. Immunol. 23*, 319−330.

Young, R. J., Owens, R. J., Mackay, G. A., Chan, C. M. W., Shi, J., Hide, M., Francis, D. M., Henry, A. J., Sutton, B. J., & Gould, H. J. (1995) *Protein Eng. 8*, 193−199.

Zheng, Y., Shopes, B., Holowka, D., & Baird, B., (1991) *Biochemistry 30*, 9125−9132.

BI971299+